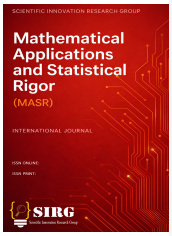

Mathematical Applications and Statistical Rigor
MASR

Journal Homepage
https://pub.scientificirg.com/index.php/MASR/index

Spectral Analysis of Long Memory in Financial Volatility Dynamics: Evidence from the CAC 40 Stock Market Index

Barkahoum Laala[a] [1]

[a] *Department of Mathematics, Faculty of Exact Sciences, Constantine 1 Mentouri Brothers University, Algeria*

ABSTRACT

Long-memory processes are widely used in time series analysis to characterize persistent dependence structures over time. In financial markets, this phenomenon is particularly relevant for modeling volatility dynamics, which measure the variability and risk of asset returns. This study investigates the presence of long-memory behavior in financial volatility using a spectral analysis approach. While the persistence of volatility is a well-documented stylized fact in financial econometrics, traditional time-domain models such as ARCH, GARCH, and their extensions primarily capture short- and medium-term dependence in conditional variance, often failing to fully account for long-range dependence. This paper addresses this gap by employing a frequency-domain approach based on spectral analysis to detect long memory in volatility dynamics. The empirical study is conducted using daily data from the CAC 40 stock market index. The price series is transformed into logarithmic returns, with volatility proxied by squared returns. A comparative analysis between returns and squared returns reveals that returns exhibit weak autocorrelation, whereas squared returns display strong persistence—consistent with established stylized facts. To further examine this persistence, we perform spectral density analysis and a simulation study. The results reveal a significant concentration of spectral power at low frequencies, providing strong evidence of long-memory dynamics in volatility. These findings have important implications for volatility forecasting, risk management, and the specification of econometric models in financial applications.

PAPER INFORMATION

HISTORY

Received: 2 December 2025
Revised: 15 February 2026
Accepted: 5 March 2026
Online: 10 March 2026

MSC

62M10
62M15
62P05
91G70

KEYWORDS

Spectral analysis
Volatility modeling
Long memory
CAC 40 index

[1]Corresponding author at Department of Mathematics, Faculty of Exact Sciences, Constantine 1 Mentouri Brothers University, Algeria. E-mail: berkahoum.laala@umc.edu.dz

1 Introduction

Long-memory processes play a fundamental role in the analysis of time series characterized by persistent dependence structures over long horizons. Such processes exhibit slowly decaying autocovariance functions (ACF) and significant correlations between distant observations. This phenomenon, known as long-range dependence, has been widely documented in several disciplines including finance, economics, hydrology, and telecommunications. From a theoretical standpoint, long memory can be naturally characterized in the frequency domain through the behavior of the spectral density function (SDF) near the origin [1, 2, 3]. In particular, long-memory processes are associated with a divergence of the spectral density at low frequencies, reflecting the dominance of long-term components in the series dynamics. This representation provides an important framework for understanding persistence and dependence structures in stochastic processes [4, 5, 6, 7, 8, 9, 10, 11, 12].

In financial econometrics, modeling volatility dynamics remains a major challenge due to the presence of several well-known stylized facts in asset returns, including volatility clustering, heavy tails, and persistent dependence structures. Traditional approaches rely primarily on time-domain models such as the Autoregressive Conditional Heteroskedasticity (ARCH) model introduced by Engle [13] and its extension, the Generalized ARCH (GARCH) model proposed by Bollerslev [14]. Although these models successfully capture short-term conditional heteroskedasticity, they often fail to adequately represent long-range dependence in volatility processes. Traditional models, such as GARCH and its extensions, have become standard tools for modeling conditional volatility [15, 16, 17]. The squared returns series often used as a volatility dynamic, frequently display this property. This empirical feature provides a theoretical justification for using the A Fractionally Integrated GARCH (FIGRCH) model to capture the hyperbolic decay of volatility shocks and the long-memory behavior frequently observed in financial time series [18].

An alternative perspective for studying dependence structures in time series is provided by frequency-domain analysis. Spectral methods focus on the distribution of variance across different frequencies and are particularly effective for detecting long-memory behavior through the concentration of spectral power near the zero frequency. Despite their strong theoretical foundation, spectral approaches remain less frequently used in empirical financial modeling compared with time-domain likelihood-based methods. One of the main challenges lies in obtaining reliable estimates of the spectral density, especially when the data exhibit complex dependency structures or finite-sample distortions.

Recent methodological developments have shown that combining spectral analysis with modern data-analysis techniques can significantly improve the estimation of dependency structures in time series. In particular, Laala et al.[19] proposed an integrated framework that combines clustering and sequential analysis to improve spectral density estimation (SDE) and to reveal hidden dependency structures in time series data. This approach identifies representative patterns in the data and enhances the stability of SDE by exploiting structural similarities among observations. In a related direction, the concept of input–output space-filling representative points has been introduced as an efficient strategy for selecting informative subsets of observations for clustering, modeling, and statistical estimation. By constructing representative points [20, 21, 22] that adequately cover the input–output space, this methodology allows a more efficient representation of complex stochastic systems and improves the robustness of statistical inference in high-dimensional settings.

Motivated by these developments, this paper investigates the persistence of financial volatility within a spectral analysis framework. The objective is to analyze whether the observed persistence in volatility measures corresponds to genuine long-memory dynamics or may instead result from alternative phenomena such as structural changes or regime shifts. Using daily observations of the CAC 40 stock market index, we examine the statistical properties of returns and squared returns, analyze their ACF and SDF characteristics, and estimate the long-memory parameter using known semi-parametric spectral methods [23].

DOI: 10.1234/sirg.esit.x.x.x Laala, 2026, MASR, VOL. 1,NO. 2, PP. 107–126

The objective of this paper is to develop a comprehensive spectral framework for modeling financial volatility and to assess whether the observed persistence in volatility index reflects genuine long memory or alternative phenomena such as structural breaks or regime shifts. The spectral properties analyzes of squared returns derive the frequency-domain implications of fractional volatility models, and employ semi-parametric spectral estimators to measure the degree of long-range dependence.

The remainder of the paper is organized as follows. Section 2 presents the theoretical background on spectral analysis and long-memory processes. Section 3 introduces the volatility modeling framework including ARCH, GARCH, and FIGARCH models. Section 4 describes the empirical analysis based on CAC 40 data and reports the main statistical results. Section 5 concludes and discusses directions for future research.

2 Spectral Methods for Detecting Long Memory in Time Series

Let $\{X_t\}_{t\in\mathbb{Z}}$ be a weakly stationary stochastic process defined on a probability space (Ω, F, P), with finite second moment $E(X_t^2) < \infty$. Denote by

$$\gamma(k) = Cov(X_t, X_{t+k}) = E(X_t X_{t+k}) - E(X_t)E(X_{t-k}),$$

the ACF of X_t. By the Herglotz Theorem [24], there exists a non-decreasing bounded function $F(\lambda)$ such that

$$\gamma(k) = \int_{-\pi}^{\pi} e^{ik\lambda} dF(\lambda).$$

If $F(\lambda)$ is absolutely continuous, then $dF(\lambda) = f(\lambda)d\lambda$, where $f(\lambda)$ is the SDF. By Fourier inversion, f is given by

$$f(\lambda) = \frac{1}{2\pi} \sum_{k=-\infty}^{\infty} \gamma(k) e^{-ik\lambda}, \quad \lambda \in [-\pi, \pi], \tag{1}$$

where λ is the frequency and h is the lag in time. The SDF provides a complete characterization of second-order properties of X_t. In particular, the behavior of $f(\lambda)$ near zero frequency reflects the persistence structure of the process.

A stationary process said to exhibit long memory (or long-range dependence) property, in time domain, if its ACF are not absolutely summable:

$$\sum_{k=-\infty}^{\infty} |\gamma(k)| = \infty.$$

The corresponding behavior asymptotic is given by

$$\gamma(k) \sim C_\gamma k^{d-1}, \quad as\ k \to \infty. \tag{2}$$

Therefore, the ACF implies a hyperbolic decay. In contrast, the short-memory processes is exponential decay:

$$\gamma(k) \sim C_\gamma \rho^k, \quad as\ k \to \infty,\ with\ 0 < \rho < 1.$$

The spectral approach provides an alternative and useful way to describe persistence and dependence structures in time series. Long memory can also be characterized through the behavior near the zero frequency of the SDF. The SDF of a stationary process is defined by 1 and using the asymptotic behavior 2 we obtain

$$f_X(\lambda) \approx \sum_{k=1}^{\infty} k^{d-1} C_\gamma \cos(k\lambda).$$

DOI: 10.1234/sirg.esit.x.x.x

This sum is the Fourier transform of a regularly varying sequence [25]. Applying classical Abelian–Tauberian theorems for Fourier series [26], we obtain

$$f(\lambda) \sim C_f |\lambda|^{-d}, \quad \lambda \to 0, \tag{3}$$

where $C_f > 0$ is a constant depend to SDF, λ is the frequency, and d is the long-memory parameter. Thus, long memory in the time domain corresponds to a divergence of the SDF at low frequencies. This property was originally discussed in the long-memory literature by [9]. When $0 < |d| < 1$, the SDF diverges near the zero frequency, indicating that low-frequency components dominate the spectrum. This behavior reflects strong persistence and long-range dependence in the series [7, 8, 24, 11, 12, 23, 32, 33].

The persistence property of memory [27, 28, 1] is determined by:

- $d = 0$ is short memory stationary process,
- $0 < |d| < 1$ is long memory stationary process, and
- $|d| \geq 1$ is non-stationary behavior.

The autoregressive-moving average (ARMA) model is a well-known process that has a short memory property when $d = 0$.

The divergence of the SDF at low frequencies indicates that the process is dominated by low-frequency components. In practical terms, this means that shocks affecting the series decay very slowly over time. Consequently observations that are far apart in time may still exhibit significant dependence. This behavior is known as *long-range dependence* or *long memory*. Therefore, the SDF provides an important tool for detecting and analyzing long-memory behavior in time series data. After analyzing the long-memory properties of the time series, the spectral density estimator (SDE) is defined using two classical nonparametric methods: the Periodogram estimator (PE) and the lag-window estimator (LWE).

Let X_t, $t = 1, \ldots, n$, be a stationary time series with mean zero. The PE of the spectral density at frequency λ is defined as

$$I_n(\lambda) = \frac{1}{2\pi n} \left| \sum_{t=1}^{n} X_t e^{-i\lambda t} \right|^2, \quad where \quad i = \sqrt{-1} \ \ and \ \ \lambda \in [-\pi, \pi]. \tag{4}$$

The PE provides a direct estimate of the SDF obtained from the discrete Fourier transform of the time series. However, although it is asymptotically unbiased, it is not a consistent estimator because its variance does not decrease with the sample size. Consequently, the PE is often used as a preliminary tool for identifying dominant frequency components in the data.

To obtain a consistent estimate of the spectral density, the LWE is commonly used. This estimator is based on the sample ACFs and applies a smoothing kernel to reduce the variability of the spectral estimate. Let $\hat{\gamma}(k)$ denote the sample ACF at lag (k)

$$\hat{\gamma}(k) = \frac{1}{n} \sum_{t=1}^{n-|k|} (X_t - \bar{X}_t)(X_{t+|k|} - \bar{X}_{t+k}), \quad with \ \ \bar{X}_t = \frac{1}{n} \sum_{t=1}^{n} X_t.$$

The LWE is one of the SDE methods, it is defined as follows

$$\hat{f}(\lambda) = \frac{1}{2\pi} \sum_{k=-M}^{M} w\left(\frac{k}{M}\right) \hat{\gamma}(k) e^{-i\lambda k}, \tag{5}$$

DOI: 10.1234/sirg.esit.x.x.x

where $w(\cdot)$ is a window (kernel) function, M is the truncation lag (bandwidth) controlling the amount of smoothing [1, 23, 29]. The LWE reduces the variance of the PE by smoothing the sample ACFs, producing a more stable estimate of the SDF.

Consider the ARMA (p, q) process defined by

$$\Phi(L)X_t = \Theta(L)\epsilon_t,$$

where: L is the lag operator, $\Theta(L)$ and $\Phi(L)$ are polynomials, ϵ_t is white noise with variance σ^2. The usual extension of ARMA process is the Fractionally Integrated ARMA (ARFIMA) (p, d, q) process given by

$$\Phi(L)(1 - L)^d X_t = \Theta(L)\epsilon_t.$$

The fractional differencing operator is defined by

$$(1 - L)^d = \sum_{k=0}^{\infty} C_d^k (-L)^k, \quad where \quad C_d^k = \frac{\Gamma(k + 1)}{\Gamma(d - k + 1)\Gamma(d + 1)}.$$

The spectral density of an ARFIMA process behaves near zero as:

$$f(\lambda) \approx \frac{\sigma^2}{2\pi} |\lambda^{-d}| \left| \frac{\Phi(e^{-i\lambda})}{\Theta(e^{-i\lambda})} \right|^2.$$

Hence, the long-memory behavior is entirely governed by the fractional parameter d [30, 31].

3 A Stochastic Framework for Financial Volatility Dynamics with Long Memory

Financial time series are usually characterized by strong variability and time–varying volatility. In empirical finance, the analysis is generally performed on asset returns rather than prices because price series are typically non–stationary.

Let P_t denote the price of a financial asset at time t. The logarithmic return series is defined as

$$r_t = \log\left(\frac{P_t}{P_{t-1}}\right), \tag{6}$$

where P_t is the asset price at time t, P_{t-1} is the price at time $t - 1$, and r_t is the return observed at time t. The logarithmic return measures the relative change in price between two consecutive periods. Log–returns are widely used because they possess important statistical properties such as approximate additivity over time and improved stationarity compared to raw prices. For small variations in prices, the logarithmic return (6) can be approximated using the first-order Taylor expansion of the logarithm function, $\log(1 + x) \approx x$. Hence

$$r_t \approx \frac{P_t - P_{t-1}}{P_{t-1}}.$$

This approximation shows that the return corresponds to the percentage change in the asset price.

The return series $\{r_t\}$ can be decomposed into two components: a predictable component and an unpredictable innovation. This decomposition is written as

$$r_t = \mu_t + \varepsilon_t, \tag{7}$$

where

- μ_t is the conditional mean of the return,

DOI: 10.1234/sirg.esit.x.x.x Laala, 2026, MASR, VOL. 1,NO. 2, PP. 107–126

- ε_t is the innovation or error term.

The conditional mean represents the expected return given the information available up to time $t-1$.

$$\mu_t = E(r_t \mid \mathcal{F}_{t-1}).$$

Here $\mathcal{F}_{t-1}$ denotes the information set available at time $t-1$. This set typically contains past returns, past errors, and other relevant historical information. Therefore, μ_t represents the best forecast of r_t based on past information.

A common specification for modeling the conditional mean is the ARMA(p,q) model:

$$\mu_t = c + \sum_{i=1}^{p} \phi_i r_{t-i} + \sum_{j=1}^{q} \theta_j \varepsilon_{t-j}, \tag{8}$$

where c is a constant, ϕ_i are autoregressive coefficients, θ_j are moving average coefficients. The autoregressive (AR) part captures the influence of past returns on the current return (r_t), while the moving average (MA) component captures the impact of past shocks (ε_{t-j}). By substituting μ_t into the return equation 7, we obtain

$$r_t = c + \sum_{i=1}^{p} \phi_i r_{t-i} + \sum_{j=1}^{q} \theta_j \varepsilon'_{t-j} + \varepsilon_t. \tag{9}$$

This equation describes the dynamics of the return process. A simple example is the ARMA(1,1) model:

$$r_t = c + \phi_1 r_{t-1} + \theta_1 \varepsilon'_{t-1} + \varepsilon_t.$$

In this case, the current return r_t depends on the previous return r_{t-1}, the previous shock ε'_{t-1}, and a new innovation ε_t.

In classical time series models, the innovation process ε_t is assumed to follow a white noise process.

- Zero Mean: $E(\varepsilon_t) = 0$. This property ensures that the innovations do not introduce systematic bias into the model.
- Constant Variance $Var(\varepsilon_t) = \sigma^2$. This assumption implies that the variance of the error term remains constant over time.
- No Autocorrelation $Cov(\varepsilon_t, \varepsilon_{t-k}) = 0, \quad k \neq 0$. This means that innovations are independent over time. A stronger assumption is that the innovations follow a Gaussian distribution $\varepsilon_t \sim N(0, \sigma^2)$.

Financial returns often violate the constant variance assumption. Three important empirical features are commonly observed:

- Volatility clustering means that large price changes tend to be followed by large changes, while small changes are followed by small changes. This phenomenon implies that

$$Var(\varepsilon_t \mid \mathcal{F}_{t-1}) \textit{ is not constant over time.} \tag{10}$$

- Heavy tails indicate that extreme events occur much more frequently than would be expected in a normal distribution. Thus, the assumption of Gaussian white noise significantly underestimates extreme risks.

DOI: 10.1234/sirg.esit.x.x.x Laala, 2026, MASR, VOL. 1,NO. 2, PP. 107–126

- Leverage effects the asymmetric response of volatility to shocks, where a negative return generally leads to a greater increase in future volatility than a positive return of the same magnitude. The leverage effect means that the conditional variance σ_t^2 (volatility) responds more strongly to a negative shock ($\varepsilon_{t-1} < 0$) than to a positive shock ($\varepsilon_{t-1} > 0$) of the same absolute size.

To capture this behavior, conditional heteroskedasticity (volatility) models are introduced. Thus, by treating ε_t as simple white noise, the ARMA model fails to account for the dynamic, predictable, and asymmetric properties of volatility—asymmetric behavior of risk— given the central role these properties play in analysis of the financial times series .

ARMA models describe the conditional mean of returns but assume constant variance, The volatility modeling is to capture the time-varying behavior of return. The framework focus on the innovation term ε_t, which represents unexpected shocks affecting financial markets. An Autoregressive Conditional Heteroskedasticity (ARCH) or Generalized ARCH (GARCH) family of models are introduced to model the conditional variance of returns. Keep the equation 7, the error term can be written as

$$\varepsilon_t = \sigma_t z_t, \tag{11}$$

where σ_t is the conditional standard deviation, z_t is an independent process with mean zero and variance one. Therefore, in accordance with property 10, we have

$$Var(\varepsilon_t|\mathcal{F}_{t-1}) = \sigma_t^2.$$

The goal of volatility models is therefore to describe the evolution of σ_t^2.

The ARCH(q) model proposed by Engle [13] defines the conditional variance σ_t^2 as

$$\sigma_t^2 = \omega + \alpha_1\varepsilon_{t-1}^2 + \alpha_2\varepsilon_{t-2}^2 + \cdots + \alpha_q\varepsilon_{t-q}^2.$$

This specification implies that the current volatility depends on past squared shocks. A large shock ε_t in the past increases the current conditional variance. This creates volatility clustering. The model finally captures the fact that variance is not constant, but predictable.

Bollerslev [14] generalized the ARCH model by including past variances. The Generalized Autoregressive Conditional Heteroskedasticity Model (GARCH) GARCH(1, 1) model is defined as

$$\sigma_t^2 = \omega + \alpha\varepsilon_{t-1}^2 + \beta\sigma_{t-1}^2, \tag{12}$$

where ω(Constante) represents the long-run volatility level, α(ARCH coefficient) measures the impact of recent shocks, and β(GARCH coefficient) captures volatility persistence.

The sum $(\alpha + \beta)$ measures how persistent volatility is over time [16, 35]. The GARCH(1,1) model is the workhorse of financial econometrics. It captures volatility clustering extremely well with just three parameters.

A Fractionally Integrated GARCH (FIGRCH) model extends GARCH by allowing long memory behavior in volatility dynamics, it was introduced by Baillie et al.[5]. The general representation is

$$\phi(L)(1-L)^d\varepsilon_t^2 = \omega + [1-\beta(L)]v_t, \tag{13}$$

with $v_t = \varepsilon_t^2 - \sigma_t^2$, L is the lag operator, and d is the fractional integration parameter. The lag polynomials are defined as

$$\phi(L) = 1 - \phi_1 L - \ldots - \phi_p L^p, \quad \beta(L) = \beta_1 L + \ldots + \beta_q L^q,$$

DOI: 10.1234/sirg.esit.x.x.x

The roots of $\phi(L)$ lie outside the unit circle to ensure stability. The fractional differencing operator $(1-L)^d$ is defined as

$$(1-L)^d = \sum_{k=0}^{\infty} \frac{\Gamma(k-d)}{\Gamma(-d)\Gamma(k+1)} L^k = \sum_{k=0}^{\infty} \pi_k L^k. \tag{14}$$

For large k, the coefficients satisfy $\pi_k \sim \frac{k^{d-1}}{\Gamma(d)}$, which implies a hyperbolic decay rather than an exponential one.

This infinite expansion implies that past shocks decay slowly, which generates long–range dependence in volatility. Several well-known volatility models arise as special cases, such as the value of d determines the degree of persistence:

- $d = 0$ corresponds to the GARCH model,
- $d = 1$ corresponds to the non stationary GARCH model,
- $0 < d < 1$ indicates long memory (strong persistence) in the volatility process.

The FIGARCH model admits the following infinite ARCH representation, from formula 13 and 14 and under finite fourth moments of ε_t $(E(\varepsilon_t^4) < \infty)$, the σ_t^2 admits an infinite-order representation:

$$\sigma_t^2 = \sum_{k=0}^{\infty} \pi_k \varepsilon_{t-k}^2.$$

Then, for ε_t^2 is independent of past volatility and $E(\varepsilon_t^4) < \infty$, the ACF of σ_t^2 satisfies

$$\gamma_{\sigma^2}(k) = Cov(\sigma_t^2, \sigma_{t+k}^2) \sim Ck^{d-1}, \qquad k \to \infty.$$

From formula 2 and for $(0 < d < 1)$, ACF of σ_t^2 decay hyperbolically. Then, the ACF of the conditional variance satisfies the long rang dependence structure

4 Long Memory in CAC 40 Volatility: An Empirical Investigation

This section presents an empirical investigation of long-memory behavior in financial volatility using daily observations of the CAC 40 stock market index. The CAC 40 is determined by selecting the 40 companies out of 100 that generate the highest trading volume on Euronext Paris. The list of companies listed on the CAC 40 is reviewed regularly to maintain a degree of representation across different sectors. CAC originally stood for Compagnie des Agents de Change, but today the acronym stands for Cotation Assistée en Continu (Continuous Assisted Quotation).

The objective of this simulation study is to examine whether volatility dynamics exhibit persistent dependence structures consistent with fractional integration for real data. The empirical analysis is structured as follows: First, the data and transformation procedures are described. Second, preliminary statistical properties of the series are analyzed. Third, the dependence structure of returns r_t and squared returns r_t^2 is examined using ACF and SDF analysis.

DOI: 10.1234/sirg.esit.x.x.x

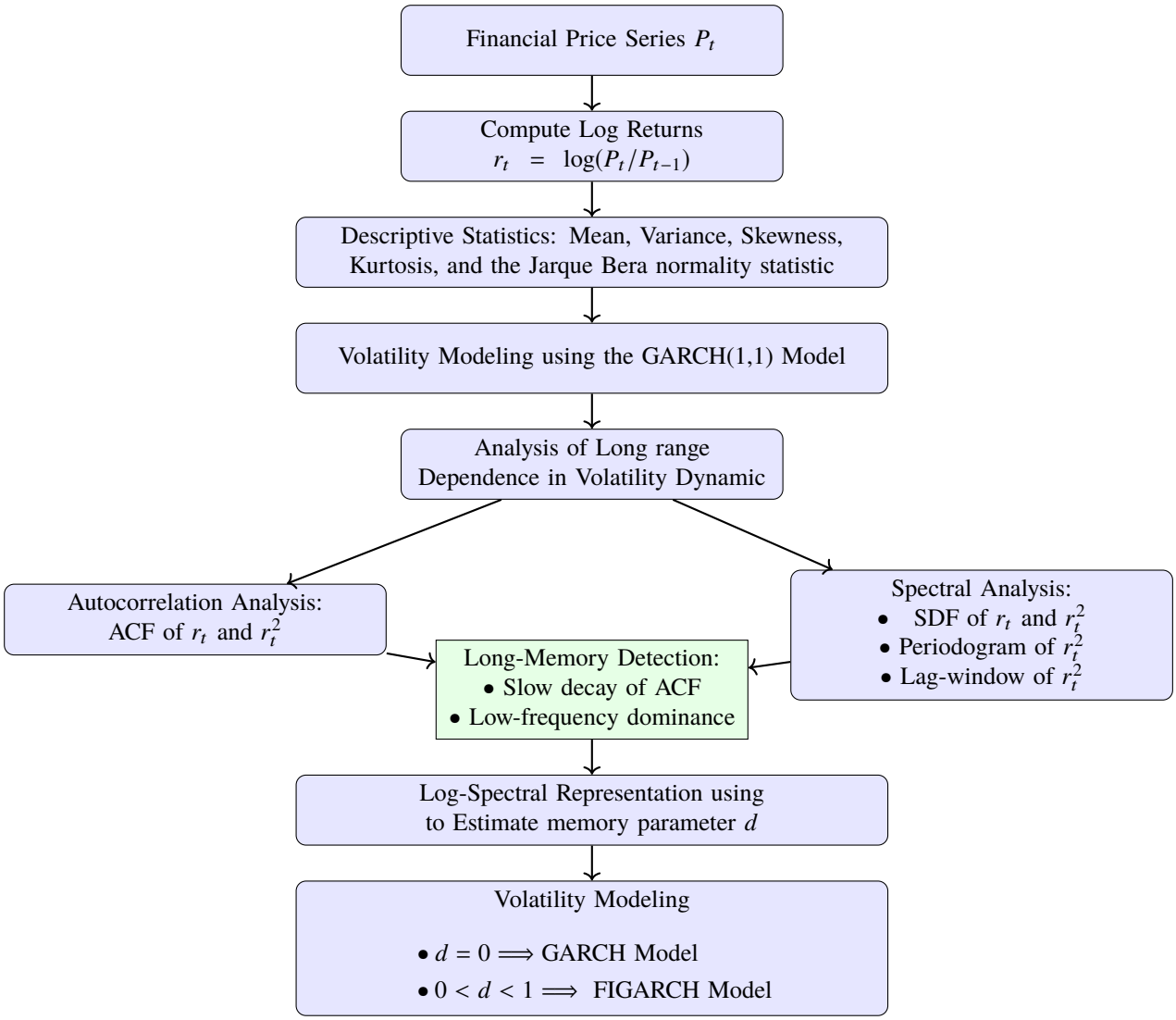

Figure 1: Flowchart of the empirical methodology used to analyze Volatility Dynamic and long-memory behavior in financial time series .

4.1 Description Analysis of the Price and Return Series

The empirical analysis uses daily observations of the CAC 40 index covering the period from January 1, 1996 to December 31, 2015. The CAC 40 index represents the forty largest companies listed on the Paris stock exchange and serves as the benchmark index for the French equity market. Logarithmic returns r_t are widely used in financial econometrics because they possess desirable statistical properties such as approximate additivity over time and improved stationarity compared to raw prices p_t. Figures 2 and 3 represent the evolution of the CAC 40 price series p_t and the corresponding return series r_t in formula 3. Figure 2 shows that the price series is non-stationary and characterized by large fluctuations and long-term growth trends. Such behavior is typical of financial price series. Figure 3 illustrates the return series r_t, which fluctuates around zero and appears approximately stationary

DOI: 10.1234/sirg.esit.x.x.x

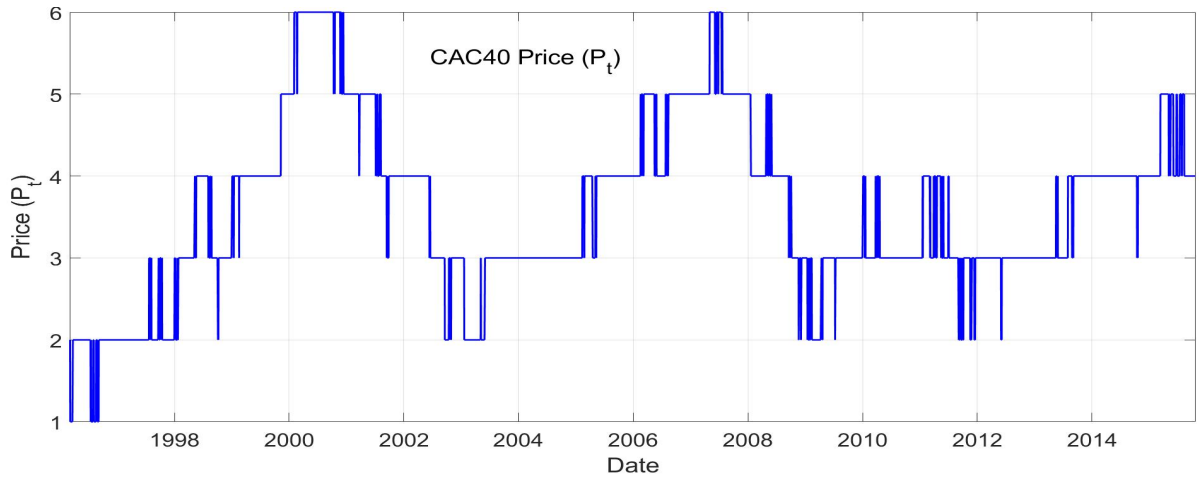

Figure 2: The price series of CAC 40 data

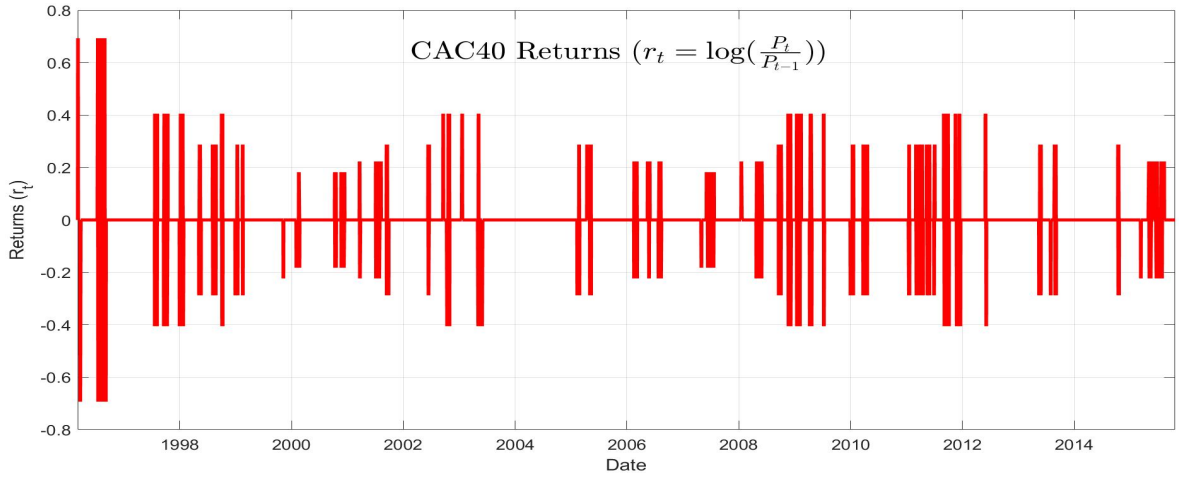

Figure 3: The correspondence return of the price of the CAC 40

4.2 Statistics and Normality Test of the Return and square Return

This subsection presents the descriptive statistics of the CAC 40 return series in order to characterize the main distributional properties of the data before conducting the volatility analysis. These statistics provide preliminary evidence on the behavior of financial returns and allow us to verify whether the empirical data exhibit the well-known stylized facts of financial time series, such as heavy tails, asymmetry, and non-normality.

The main descriptive measures used in the analysis are the sample Mean ($\overline{r_t}$), Variance (σ^2), Stander deviation (σ), Skewness (S) , Kurtosis(K), and the Jarque Bera (J-B) normality statistic. These quantities are defined as follows:

$$\begin{cases} \text{Mean} == \frac{1}{n}\sum_{t=1}^{n} r_t, \quad \sigma^2 = \frac{1}{n}\sum_{t=1}^{n}\left(r_t - \overline{r_t}\right)^2, \quad S = \frac{1}{n}\sum_{t=1}^{n}\left(\frac{r_t-\overline{r_t}}{\sigma}\right)^3, \\ K = \frac{1}{n}\sum_{t=1}^{n}\left(\frac{r_t-\overline{r_t}}{\sigma}\right)^4, \quad \text{J-B} = \frac{n}{6}\left(S^2 + \frac{(K-3)^2}{4}\right). \end{cases}$$

These statistics respectively measure the central tendency of the returns, their dispersion, the asymmetry of the distribution, and the thickness of the distribution tails.

The Jarque–Bera statistic is a widely used test for normality [34]. It jointly evaluates whether the Skewness and Kurtosis of the sample are consistent with those of a normal distribution.

DOI: 10.1234/sirg.esit.x.x.x Laala, 2026, MASR, VOL. 1,NO. 2, PP. 107–126

The hypotheses of the test are defined as follows:

$$H_0 : r_t \sim \text{Normal Distribution}, \quad H_1 : r_t \nsim \text{Normal Distribution}$$

Under the null hypothesis H_0, the Jarque–Bera statistic asymptotically follows a chi-squared distribution with two degrees of freedom:

$$JB \sim \chi^2(2), \quad \text{the corresponding p-value is computed as} \quad p\text{-value} = 1 - F_{\chi^2(2)}(JB),$$

where $F_{\chi^2(2)}$ denotes the cumulative distribution function of the chi-squared distribution with two degrees of freedom. The decision rule is defined as follows:

- If p-value $> \alpha$ (typically $\alpha = 0.05$), H_0 cannot be rejected and the data may be considered normally distributed.
- If p-value $\leq \alpha$, H_0 is rejected, indicating that the distribution significantly deviates from normality.

Table 1: Descriptive Statistics of Returns, Square Return, and Absolute Return

Series	n	Mean	σ	S	K	J-B
r_t (Returns)	4999	-0.00014	0.07236	-0.042	35.42	2.19×10^5
r_t^2 (Squared)	4999	0.00524	0.03072	9.573	124.95	3.17×10^6
$\lvert r_t \rvert$ (Absolute)	4999	0.01484	0.07082	5.293	33.90	2.22×10^5

Note: All p-values for Jarque-Bera test are < 0.001, rejecting normality.

The high kurtosis indicates heavy tails and volatility clustering.

Table 1 reports the descriptive statistics of the CAC 40 return, squared return and absolute return series. The results of the Table 1 show

- The Mean of the return series $\overline{r_t}$ is close to zero, which is a typical feature of high-frequency financial returns. This indicates that positive and negative price movements tend to cancel out over time.
- The standard deviation σ reflects the overall volatility of the series. The relatively large value confirms that financial markets are characterized by substantial fluctuations.
- The skewness coefficient S is negative, indicating that the distribution of returns is slightly left-skewed. This suggests that extreme negative returns occur more frequently than extreme positive returns.
- The kurtosis K is significantly larger than the value of three associated with the normal distribution. This indicates the presence of heavy tails in the return distribution, meaning that extreme events occur more frequently than predicted by a Gaussian model.
- The Jarque–Bera statistic JB strongly rejects the null hypothesis of normality. This result confirms that financial returns exhibit non-Gaussian behavior, which is consistent with the stylized facts widely documented in financial econometrics.

These results are consistent with the stylized facts widely documented in financial econometrics and justify the use of conditional heteroskedastic models such as ARCH, GARCH, and FIGARCH to capture the dynamic behavior of financial volatility.

DOI: 10.1234/sirg.esit.x.x.x Laala, 2026, MASR, VOL. 1,NO. 2, PP. 107–126

4.3 A GARCH(1,1) Model to Capture the Volatility Dynamics of CAC 40 Returns

Based on the previous results, we estimate a GARCH(1,1) model to capture the volatility dynamics of CAC 40 returns. The model specification is given in Eq. (12), and the estimation results are reported in Table 2.

Table 2: GARCH(1,1) Estimation Results for CAC 40 Return Volatility

Parameter	**Value**	**SE**	**T-statistic**	**P-value**
Constant (ω)	0.00038358	5.8465e-06	65.609	0
GARCH(1) (β)	0.75511	0.0035099	215.14	0
ARCH(1) (α)	0.1972	0.0084801	23.255	1.264e-119

The results reported in Table 2 indicate that all estimated parameters are highly statistically significant. The accuracy of each parameter is measured by the *standard error* (SE), defined as

$$SE(\hat{\theta}_i) = \sqrt{\text{Var}(\hat{\theta}_i)}, \quad i = \{\omega, \beta, \alpha\},$$

which represents the standard deviation of the estimator and measures the precision of the estimated parameter. The statistical significance of each parameter is evaluated using the *t-statistic*, defined as

$$t = \frac{\hat{\theta}_i}{SE(\hat{\theta}_i)}, \quad i = \{\omega, \beta, \alpha\}.$$

This statistic is used to test the hypotheses

$$H_0 : \theta_i = 0 \qquad \text{against} \qquad H_1 : \theta_i \neq 0.$$

The corresponding *p-value* represents the probability of obtaining a t-statistic at least as extreme as the observed value under the null hypothesis. If the p-value is lower than the conventional significance level (5%), the null hypothesis is rejected. In Table 2, all p-values are close to zero, confirming that the estimated parameters are statistically different from zero.

• The ARCH coefficient ($\alpha = 0.1972$) captures the short-run impact of recent shocks on volatility, indicating that new market information significantly affects the volatility of CAC 40 returns.

• The GARCH coefficient ($\beta = 0.7551$) reflects the persistence of past volatility, suggesting that previous volatility strongly influences current volatility levels.

• Volatility persistence is measured by the sum $\alpha + \beta = 0.9523$, which is close to unity. This indicates a high degree of persistence in the volatility process of CAC 40 returns, implying that volatility shocks dissipate slowly over time, a characteristic feature of financial markets known as volatility clustering [35].

• Finally, the stationarity condition of the GARCH model ($\alpha + \beta < 1$) is satisfied, ensuring that the conditional variance remains stable in the long run. However, the high persistence may indicate the presence of long-memory effects, suggesting that alternative specifications such as the FIGARCH model could better capture the long-term volatility dynamics of the CAC 40 index.

4.4 Autocorrelation Analysis of Returns and Volatility

To examine the persistence structure of the series, the ACF is computed for both the r_t and the squared return series, then the cross correlation betweenr_t and r_t^2. The empirical ACF values are reported in Tables 3 and 4 for different lag orders. The results of Table 3 reveal an important contrast between returns and volatility:

DOI: 10.1234/sirg.esit.x.x.x Laala, 2026, MASR, VOL. 1,NO. 2, PP. 107–126

- The ACFs of the r_t are generally small and rapidly decay toward zero.
- The ACFs of the r_t^2 remain positive and significant over a large number of lags.
- The cross correlation between r_t and r_t^2

From Table 4, the decay pattern of the ACF of r_t^2 is slow and gradual rather than exponential. Such a hyperbolic decay pattern is consistent with the theoretical behavior of long-memory processes . This result provides preliminary evidence that the volatility process may exhibit long-range dependence. Figure 4 present the ACF of the returns r_t and square returns r_t^2. Unlike the return r_t, the square of the return r_t^2 is generally strongly autocorrelated.

However, periods of high volatility alternate with periods of low volatility, indicating the presence of volatility clustering, one of the most important stylized facts of financial markets. Volatility is typically not directly observable, a common technique used in empirical studies is the squared return: $X_t = r_t^2$. Even when returns r_t themselves are weakly correlated, squared returns r_t^2 often display strong serial dependence, reflecting persistent volatility dynamics.

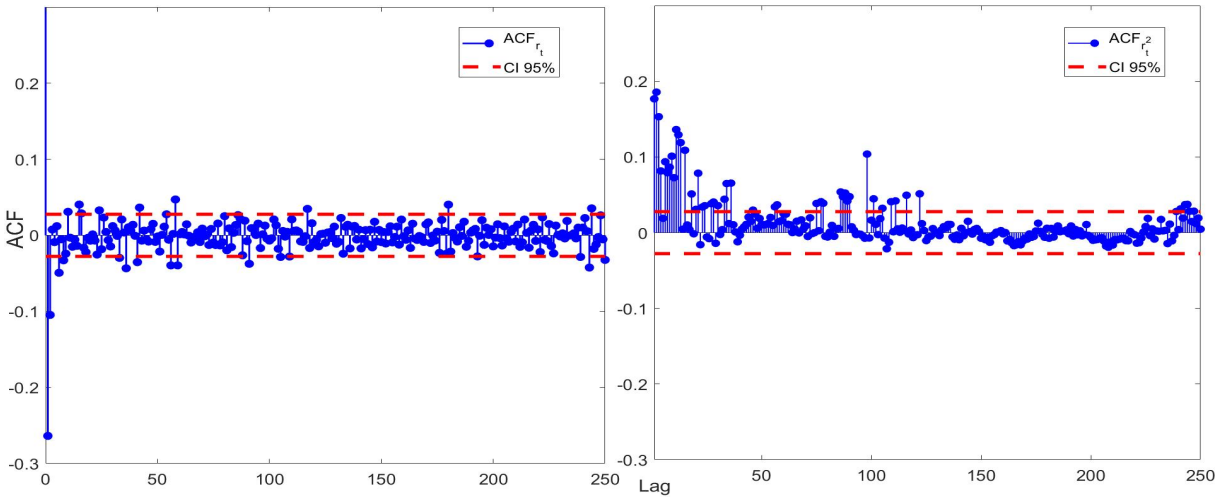

Figure 4: ACF of the returns r_t and square returns r_t^2 of CAC 40

4.5 Spectral Analysis and Long-Memory Identification

Figure 5 displays the SDF of the return series r_t and the squared return series r_t^2. The spectrum of squared returns r_t^2 shows a strong concentration of power near zero frequency, which is a characteristic feature of long-memory processes. Figure 6 presents the SDE of squared returns r_t^2 obtained from both methods PE and LWE methods, given in formula 4 and 5 respectively. The results highlight the concentration of spectral power at low frequencies, which suggests the presence of persistent volatility dynamics. The pronounced peak near the origin indicates that long-term components play a dominant role in the volatility dynamics.

The presence of long-memory behavior can be further investigated through the asymptotic behavior of the spectral density near the origin. To facilitate empirical estimation, the logarithm of the SDF can be considered. Taking logarithms of the expression 3 yields the log-spectral representation

$$\log f_X(\lambda) = \log C_f - d \log |\lambda|.$$

Differentiating with respect to $\log \lambda$ gives

$$\frac{\partial \log f_X(\lambda)}{\partial \log \lambda} = -d.$$

DOI: 10.1234/sirg.esit.x.x.x Laala, 2026, MASR, VOL. 1,NO. 2, PP. 107–126

Table 3: ACFs for Return r_t and the Square Return r_t^2, and their cross-Covariances for CAC 40 (01/01/1996 - 31/12/2015)

Lags 1-25					Lags 26-50				
h	ρ_{r_t}	$\rho_{r_t^2}$	ρ_{r_t,r_t^2}	Signif	h	ρ_{r_t}	$\rho_{r_t^2}$	ρ_{r_t,r_t^2}	Signif
1	-0.2637	0.1768	**-1.0000**	***	26	0.0233	-0.0079	0.0000	
2	-0.1046	0.1856	**-1.0000**	***	27	0.0044	0.0382	0.0900	*
3	0.0076	0.1531	0.5400	**	28	-0.0063	0.0404	-0.1350	*
4	-0.0089	0.0815	-0.3150	*	29	-0.0146	-0.0141	0.0900	*
5	0.0120	0.0189	0.0900	*	30	0.0121	0.0357	0.1800	*
6	-0.0493	0.0937	**-1.0000**	***	31	0.0064	-0.0025	0.0000	
7	-0.0052	0.0791	-0.1800	*	32	-0.0007	0.0039	-0.0000	
8	-0.0328	0.0865	**-1.0000**	***	33	-0.0296	0.0441	-0.5850	**
9	-0.0241	0.1010	**-1.0000**	***	34	0.0208	0.0649	0.6300	**
10	0.0309	0.0726	0.9900	***	35	0.0037	0.0120	0.0000	
11	-0.0031	0.1361	-0.1800	*	36	-0.0433	0.0654	**-1.0000**	***
12	-0.0150	0.1293	-0.8550	**	37	0.0105	0.0104	0.0450	
13	-0.0058	0.1190	-0.3150	*	38	0.0064	0.0009	0.0000	
14	-0.0138	0.0046	0.0000		39	0.0138	-0.0121	0.0000	
15	0.0405	0.1088	**1.0000**	***	40	-0.0006	-0.0033	0.0000	
16	0.0290	0.0101	0.1350	*	41	-0.0353	0.0047	0.0000	
17	-0.0163	0.0041	-0.0450		42	0.0365	0.0078	0.1350	*
18	-0.0222	0.0511	-0.4950	**	43	-0.0069	0.0109	-0.0450	
19	-0.0032	-0.0015	0.0000		44	0.0062	0.0206	0.0450	
20	-0.0070	0.0307	-0.0900	*	45	-0.0050	0.0150	-0.0450	
21	0.0012	0.0785	0.0450		46	-0.0082	0.0297	-0.0900	*
22	-0.0069	-0.0159	0.0450		47	0.0081	0.0245	0.0900	*
23	-0.0253	0.0339	-0.4050	*	48	0.0151	0.0058	0.0000	
24	0.0328	0.0355	0.5400	**	49	-0.0086	0.0187	-0.0900	*
25	-0.0182	-0.0058	0.0450		50	-0.0015	0.0110	-0.0000	

- Significance: *** $|\rho| > 0.9$, ** $0.5 < |\rho| \leq 0.9$, * $0.1 < |\rho| \leq 0.5$
- $\rho_{r_t,r_t^2}(h) = \frac{\text{Cov}(r_{t+h},r_t^2)}{\sigma_r \sigma_{r^2}}$ is the cross Covariance between r_{t+h} et r_t^2, normalized by $\sigma_r \sigma_{r^2} = 0.002223$
- The **bold** value indicate a correlation $|\rho| = 1$

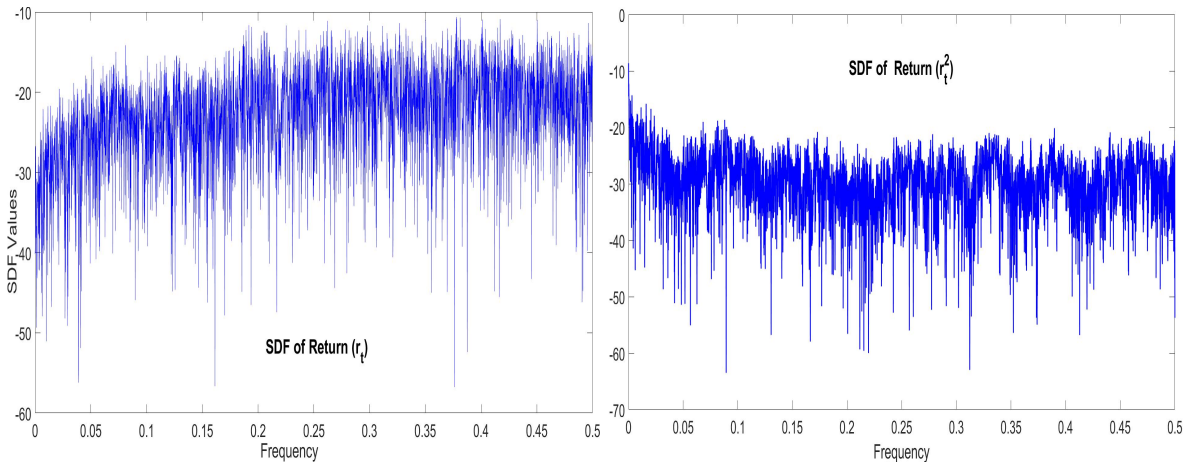

Figure 5: SDF of the returns r_t and the square return r_t of CAC 40

This relationship shows that the slope of the log-spectrum near the zero frequency corresponds to the negative value of the memory parameter. Consequently, the long-memory parameter can be estimated from the slope of the log-SDF in the low-frequency region. This property forms the basis of several semi-parametric estimators such as the log-PE or log-LWE.

Figure 7 illustrates the estimated log-SDF of the squared returns r_t^2 of the CAC 40 index. The figure exhibits an approximately linear pattern in the low-frequency region, which is consistent with the theoretical log-spectral representation of long-memory processes. The negative slope observed in the

DOI: 10.1234/sirg.esit.x.x.x

Table 4: ACF decay analysis for Return r_t and Square Return r_t^2

Lag range	Mean ACF r_t	Mean ACF r_t^2	Decay pattern
1-10	-0.0438	0.1107	Rapid decay for r_t, slow for r_t^2
11-20	-0.0019	0.0507	r_t near zero, r_t^2 still positive
21-30	-0.0008	0.0258	r_t^2 slowly decaying
31-40	-0.0016	0.0148	r_t^2 approaching zero
41-50	0.0004	0.0151	Residual positive correlation

log-spectrum indicates that the SDF decreases as the frequency increases, confirming the dominance of low-frequency components in the volatility dynamics.

From the estimated slope of the log-spectrum, the long-memory parameter is obtained as $d = 0.4429$. Since this value satisfies $(0 < d < 1)$, the volatility process can be classified as a stationary long-memory process. This result indicates that volatility shocks decay slowly and may affect future volatility over long time horizons.

The empirical findings therefore support the presence of fractional persistence in financial volatility. Standard GARCH models assume an exponential decay of shocks and may therefore be insufficient to capture such long-range dependence. Models incorporating fractional integration, such as the FIGARCH model, provide a more flexible framework capable of capturing both short-term dynamics and long-term persistence in volatility.

Overall, the empirical evidence obtained from the CAC 40 index strongly supports the presence of persistent volatility dynamics consistent with long-memory behavior. These results have important implications for volatility forecasting, financial risk management, and the specification of econometric models for financial time series.

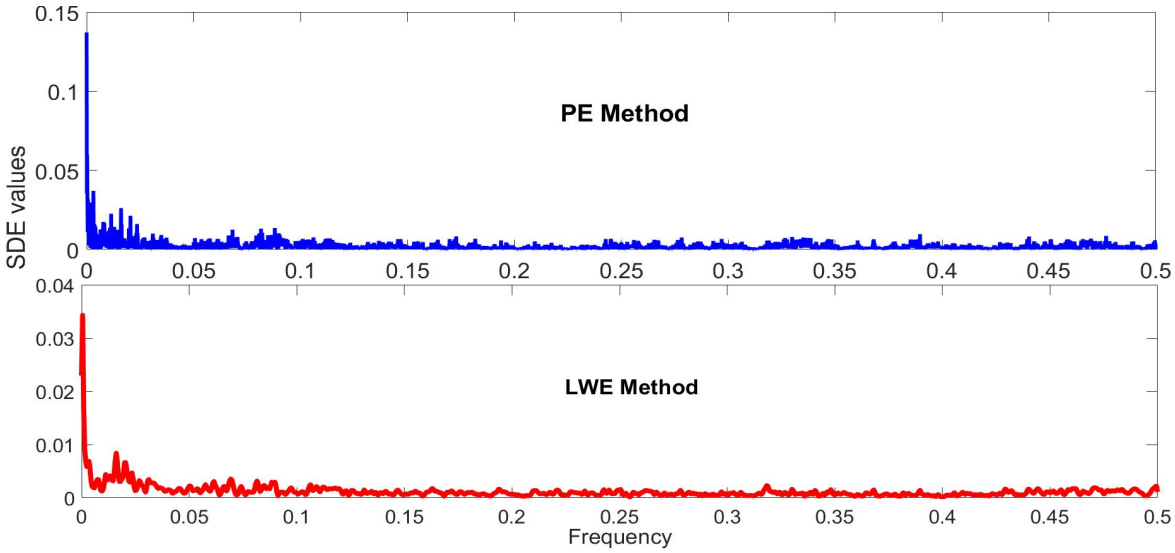

Figure 6: SDE of CAC 40 Square Returns based on the PE and LWE methods.

DOI: 10.1234/sirg.esit.x.x.x

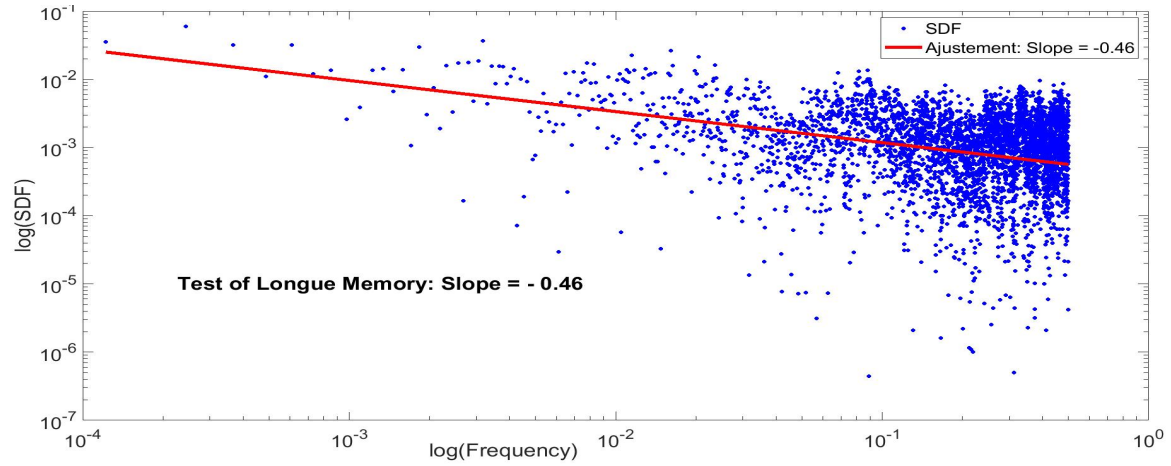

Figure 7: Log- SDF of the squared returns r_t^2 of the CAC 40 index. The approximately linear relationship between $log\, f(\lambda)$ and $log\lambda$ in the low-frequency region indicates long-memory behavior, and the slope of the curve provides an estimate of the memory parameter d.

5 Conclusion and Future Work

This study investigated the persistence of financial volatility using a spectral analysis framework combined with classical volatility modeling techniques. The objective was to examine whether the volatility dynamics of financial returns exhibit long-memory behavior and to assess the adequacy of traditional volatility models in capturing this persistence.

Using daily observations of the CAC 40 stock market index over the period 1996–2015, we analyzed the statistical properties of returns and squared returns. The empirical analysis confirmed several well-known stylized facts of financial time series, including volatility clustering, heavy tails, and significant departures from normality. While the return series itself showed weak autocorrelation, the squared return series displayed strong and persistent dependence over many lags, suggesting the presence of long-range dependence in volatility dynamics.

The analysis of the autocorrelation function revealed a slow and gradual decay for the squared returns, which is consistent with the theoretical behavior of long-memory processes. This result was further supported by the spectral density analysis, which showed a strong concentration of spectral power near the zero frequency. Such a pattern indicates that low-frequency components dominate the volatility process and provides strong evidence of persistent dynamics in the CAC 40 volatility series.

The estimated fractional parameter obtained from spectral methods was approximately $d = 0.4429$, which lies within the interval (0 < d < 1). This confirms that the volatility process can be characterized as a stationary long-memory process. These findings suggest that standard short-memory models such as GARCH may not fully capture the persistence observed in financial volatility. In contrast, fractionally integrated models such as the FIGARCH framework provide a more flexible representation of volatility dynamics by allowing a hyperbolic decay of shocks over time.

Overall, the empirical results highlight the importance of considering long-memory structures when modeling financial volatility. The combination of spectral analysis and volatility modeling provides a useful framework for detecting and quantifying persistent dependence in financial time series. These findings have important implications for volatility forecasting, portfolio risk management, and the specification of econometric models used in financial applications.

Future research may extend this work in several directions. First, more advanced spectral estimation techniques could be employed to improve the robustness of long-memory parameter estimation.

DOI: 10.1234/sirg.esit.x.x.x Laala, 2026, MASR, VOL. 1,NO. 2, PP. 107–126

Second, recent developments combining clustering methods and sequential analysis for improving spectral density estimation may provide a promising framework for identifying hidden dependency structures in time series data. Third, applying the proposed approach to other financial markets or high-frequency data could provide further insights into the nature of long-memory behavior in financial volatility. Fourth, an important avenue for future research lies at the intersection of experimental design and time series analysis. The quality and informativeness of any empirical analysis fundamentally depend on the dataset used [37, 38]. In this context, the principles of optimal experimental design can be leveraged to construct datasets that are not merely passively observed but strategically designed to capture the most relevant information about underlying processes. For instance, the concept of orthogonal designs [39], foldover designs [40], sequential designs [41], follow-up designs [42], Latin hypercube designs [43], low-aliasing designs [44], uniform designs [45, 46, 47], projection designs [48, 49], coding schemes [50], and space-filling designs [51], offers a powerful framework for selecting or constructing datasets that efficiently represent the input-output space, thereby improving the accuracy and stability of subsequent statistical inference. By integrating such design principles into the data collection or selection phase, one can enhance the detection of long-memory structures and reduce estimation uncertainty. This synergy between experimental design and time series analysis opens new possibilities for more reliable volatility modeling and risk assessment in financial applications.

Acknowledgments

The author sincerely thanks the referees, Associate Editor, and Editor-in-Chief for their valuable comments and suggestions, which have greatly improved this paper. The authors also acknowledge the use of DeepSeek for assistance in improving the English grammar and language clarity.

Disclosure statement

No potential conflict of interest was reported by the author(s).

References

[1] U. Hassler, *Time Series Analysis with Long Memory in View*. John Wiley & Sons, 2019.

[2] P.M. Robinson, "Semiparametric analysis of long-memory time series," *Annals of Statistics*, vol. 22(1), p. 515–539, 1994.

[3] D. Surgailis, H. Koul, and L. Giraitis, *Large Sample Inference For Long Memory Processes*. World Scientific, 2012.

[4] C. Agiakloglou, P. Newbold, and M. Wohar, "Bias in an estimator of the fractional difference parameter," *Journal of Time Series Analysis*, vol. 14, p. 235–246, 1993.

[5] R.T. Baillie, "Long-memory processes and fractional integration in econometrics," *Journal of Econometrics*, vol. 73, p. 5–59, 1996.

[6] J. Beran, *Statistics for Long Memory Processes*. New York: Chapman and Hall, 1994.

[7] J. Beran, R. Kulik, S. Ghosh, and Y. Feng, *Long-memory processes: Probabilistic properties and statistical methods*. London: Springer, 2013.

DOI: 10.1234/sirg.esit.x.x.x

[8] G.E.P. Box and G.M. Jenkins, *Time series analysis: forecasting and control*. San Francisco: Holden Day, 1976.

[9] C.W.J. Granger and R. Joyeux, "An introduction to long-memory time series models and fractional differencing," *Journal of Time Series Analysis*, vol. 1, p. 15–29, 1980.

[10] L. Giraitis, H.L. Koul, and D. Surgailis, *Large Sample Inference for Long Memory Processes*. Imperial College Press, 2012.

[11] U. Grenander and M. Rosenblatt, "Statistical spectral analysis of time series arising from stationary stochastic processes," *Annals of Mathematical Statistics*, vol. 24(4), p. 537–558, 1953.

[12] J.R.M. Hosking, "Fractional differencing," *Biometrika*, vol. 68(1), p. 165–176, 1981.

[13] R.F. Engle, "Autoregressive conditional heteroscedasticity with estimates of the variance of UK inflations," *Econometrica*, vol. 59, p. 987–1007, 1982.

[14] T. Bollerslev, "Generalized autoregressive conditional heteroskedasticity," *Journal of Econometrics*, vol. 31(3), p. 307–327, 1986.

[15] T. Bollerslev and R.F. Engle, "Common persistence in conditional variances," *Econometrica*, vol. 61, p. 167–186, 1993.

[16] C. Cerovecki, C. Francq, S. Hörmann, and J.M. Zakoïan, "Functional GARCH models: The quasi-likelihood approach and its applications," *Journal of Econometrics*, vol. 209(2), p. 353–375, 2019.

[17] C. Francq and J.M. Zakoian, *GARCH models: structure, statistical inference and financial applications*. John Wiley & Sons, 2019.

[18] R.T. Baillie and R.P. DeGennaro, "Stock returns and volatility," *Journal of Financial and Quantitative Analysis*, vol. 25(2), p. 203–214, 1990.

[19] B. Laala, A.M. Elsawah, G.K. Vishwakarma, and K.T. Fang, "Integrating clustering and sequential analysis for improving the spectral density estimation and dependency structure of time series," *Communications in Statistics—Simulation and Computation*, vol. 54(3), p. 889–924, 2025.

[20] A.M. Elsawah, B. Laala, and G.K. Vishwakarma, "Input-output space-filling representative points for clustering, modeling, and estimation," *Journal of Computational and Applied Mathematics*, vol. 474, p.116928, 2026.

[21] J. Lin, J. Cao, and A.M. Elsawah, "From distance to gravitation: A new perspective for improving classification, clustering, and sampling," *Journal of King Saud University – Computer and Information Sciences*, vol. 38, p. 87, 2026.

[22] A.M. Elsawah, Y.-A. Wang, and F. Tank, "Minimum energy representative points," *Journal of Computational and Applied Mathematics*, vol. 438, p. 115526, 2024.

[23] B. Laala, S. Belaloui, K.T. Fang, and A.M. Elsawah, "Improving the lag window estimators of the spectrum and memory for long-memory stationary gaussian processes," *Communications in Mathematics and Statistics*, vol. 11, p. 1–40, 2023.

[24] P.J. Brockwell and R.A. Davis, *Time Series: Theory and Methods*, 2nd ed. New York: Springer, 1991.

[25] J.B. Hamilton, *Time Series Analysis*. Princeton University Press, 1994.

DOI: 10.1234/sirg.esit.x.x.x Laala, 2026, MASR, VOL. 1,NO. 2, PP. 107–126

[26] L.M. Koopmans, *The Spectral Analysis of Time Series*. Academic Press, 1995.

[27] G. Chen, B. Abraham, and S. Peiris, "Lag window estimation of the degree of differencing in fractionally integrated time series models," *Journal of Time Series Analysis*, vol. 15(5), p. 473–487, 1993.

[28] J. Geweke and S. Porter-Hudak, "The estimation and application of long memory time series models," *Journal of Time Series Analysis*, vol. 4(4), p. 221–238, 1983.

[29] M.S. Peiris and J.R. Court, "A note on the estimation of the degree of differencing in long memory time series analysis," *Probability and Mathematical Statistics*, vol. 14(2), p. 223–229, 1993.

[30] R.L. Hunt, M.S. Peiris, and N.C. Weber, "The bias of lag window estimators of the fractional difference parameter," *Journal of Applied Mathematics and Computing*, vol. 12, p. 67–79, 2003.

[31] C. Hurvich and K. Beltrao, "Asymptotics for the low-frequency ordinates of the periodogram of a long-memory time series," *Journal of Time Series Analysis*, vol. 14(5), p. 455–472, 1993.

[32] E. Parzen, "Time series model identification and prediction variance horizon," in *Applied Time Series Analysis II*, D. Findley, Ed. New York: Academic Press, 1981, p. 415–447.

[33] M.B. Priestley, *Spectral analysis and Time Series*. New York: Academic Press, 1981.

[34] A.K. Bera and C.M. Jarque, "Model specification tests: A simultaneous approach," *Journal of Econometrics*, vol. 20(1), p. 59–82, 1982.

[35] C.S. Li, "Common persistence in conditional variance: A reconsideration," *Economic Modelling*, vol. 29(5), p. 1809–1819, 2012.

[36] R.B. Blackman and J.W. Tukey, *The measurement of power spectra from the point of view of communications engineering—Part I*. New York: Dover, 1959.

[37] A.M. Elsawah, Y.-A. Wang, Z. Chen, et al., "A sequential designing-modeling technique when the input factors are not equally important," *Computational and Applied Mathematics*, vol. 43, p. 9, 2024.

[38] A.M. Elsawah, "Constructing orthogonal maximin distance uniform projection designs for computer experiments," *Journal of Computational and Applied Mathematics*, vol. 473, p. 116902, 2026.

[39] L.C. Weng, K.T. Fang, and A.M. Elsawah, "Degree of isomorphism: a novel criterion for identifying and classifying orthogonal designs," *Statistical Papers*, vol. 64, p. 93–116, 2023.

[40] A.M. Elsawah and H. Qin, "A new look on optimal foldover plans in terms of uniformity criteria," *Communications in Statistics—Theory and Methods*, vol. 46(4), p. 1621–1635, 2017.

[41] A.M. Elsawah, "Designing uniform computer sequential experiments with mixture levels using Lee discrepancy," *Journal of Systems Science and Complexity*, vol. 32, p. 681–708, 2019.

[42] A.M. Elsawah, "Novel techniques for performing successful follow-up experiments based on prior information from initial-stage experiments," *Statistics*, vol. 56(5), p. 1133–1165, 2022.

[43] A.M. Elsawah and Y. Gong, "A new non-iterative deterministic algorithm for constructing asymptotically orthogonal maximin distance Latin hypercube designs," *Journal of the Korean Statistical Society*, vol. 52, p. 621–646, 2023.

DOI: 10.1234/sirg.esit.x.x.x

[44] A.M. Elsawah, "A powerful and efficient algorithm for breaking the links between aliased effects in asymmetric designs," *Australian & New Zealand Journal of Statistics*, vol. 59(1), p. 17–41, 2017.

[45] S.M. Celem, B. Barkahoum, G.K. Vishwakarma, and H. Qin, "Advances in uniform experimental designs: A decade selective review of algorithmic search and deterministic construction methods," *Mathematical Applications and Statistical Rigor*, vol. 1(1), p. 1–56, 2026.

[46] S.M. Celem and H. Qin, "Lower bounds of unanchored discrepancy for mixed-level U-type designs," *Mathematical Applications and Statistical Rigor*, vol. 1(1), p. 70–88, 2026.

[47] A.M. Elsawah, "Designing optimal large four-level experiments: A new technique without recourse to optimization softwares," *Communications in Mathematics and Statistics*, vol. 10, p. 623–652, 2022.

[48] A.M. Elsawah, "Level permutations and factor projections of multiple quadruple designs," *Communications in Statistics—Simulation and Computation*, vol. 53(10), p. 4893–4920, 2024.

[49] S.M. Celem. F. Tank and H. Qin, "Benchmarking low-dimensional projection uniformity in mixed two- and three-level designs," *Mathematical Applications and Statistical Rigor*, vol. 1(2), p. 89-106, 2026.

[50] A.M. Elsawah, "A novel coding scheme for generating sixteen codes from quaternary codes with applications," *Computational and Applied Mathematics*, vol. 43, p. 118, 2024.

[51] A.M. Elsawah, "Improving the space-filling behavior of multiple triple designs," *Computational and Applied Mathematics*, vol. 41, p. 180, 2022.

DOI: 10.1234/sirg.esit.x.x.x